Supporting Information

Plasmon-Enhanced Autocatalytic N-Demethylation

Tefera E. Tesema,[†] Christopher Annesley,[‡] and Terefe G. Habteyes*,[†]

[†]Department of Chemistry and Chemical Biology, and Center for High Technology Materials, University of New Mexico, Albuquerque, New Mexico 87131, USA

[‡]Air Force Research Lab, Kirtland AFB, New Mexico 87117, USA

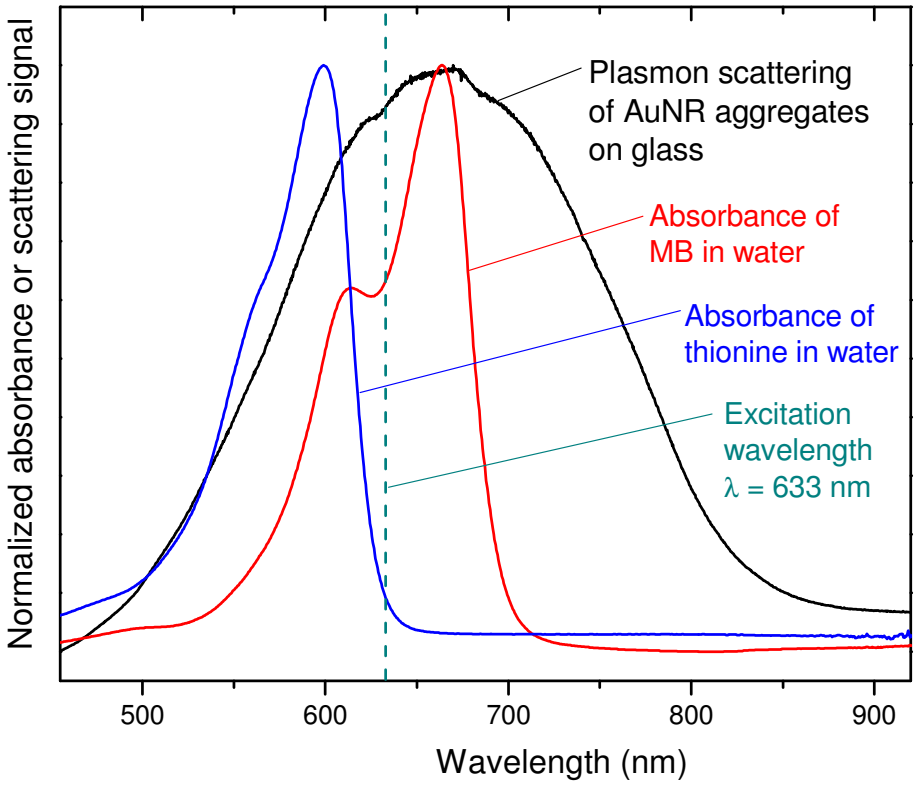

Figure S1 Spectral overlap of the excitation wavelength shown by the vertical dashed line (λ = 633 nm) with the absorption bands of methylene blue (MB) and thionine as well as with the plasmon resonances of the gold nanorods (AuNRs) aggregated on coverslip. When the molecules are adsorbed on the nanoparticles, the absorption bands are expected to broaden and red-shift as described in the main manuscript.

Analysis of SERS data – background correction

The photochemical reaction progress is monitored by recording the SERS spectra continuously as a function of exposure time. However, in addition to the vibrational signals, the fluorescence background changes with exposure time as illustrated in Figures S2 (a) and (b). To facilitate comparison of relative intensity (*I*) of vibrational bands, the fluorescence background is removed using the following relation.

$$I_{corrected}(t) = \frac{I(t) - I_b(t)}{I_b(t)} \qquad (1)$$

where $I_b(t)$ represent time dependent background signal. A flat spectral position where no vibrational bands are observed can be chosen as background signal. An example is shown in Figure S2. In Figure S2 (a), comparing the spectrum shown by the black line (acquired at 0.5 s exposure time) and that shown by the red line (acquired at 207 s of exposure time), it can be seen that the background signal is decreasing with time as plotted in Figure S2 (b). After the background correction using equation (1), the baselines of the spectra acquired at different exposure times overlap as shown in Figure S2 (c).

The SERS spectra presented in Figure S2 are obtained in N_2 atmosphere. In air and oxygen atmospheres, the background signal decreases with slightly different rates in the different regions of the spectral window as shown in Figures 2a & b. To avoid any bias this background asymmetry may cause in comparing the time dependence of different vibrational band intensities, background reference points close to the bands are used. For example, for the band at 479 cm^{-1}, the position marked as 1 in Figure S2 is used as background reference point. Similarly, position 2 is used for bands at 1392 cm^{-1} and 1435 cm^{-1}, and position 3 is used for the band at 1620 cm^{-1}.

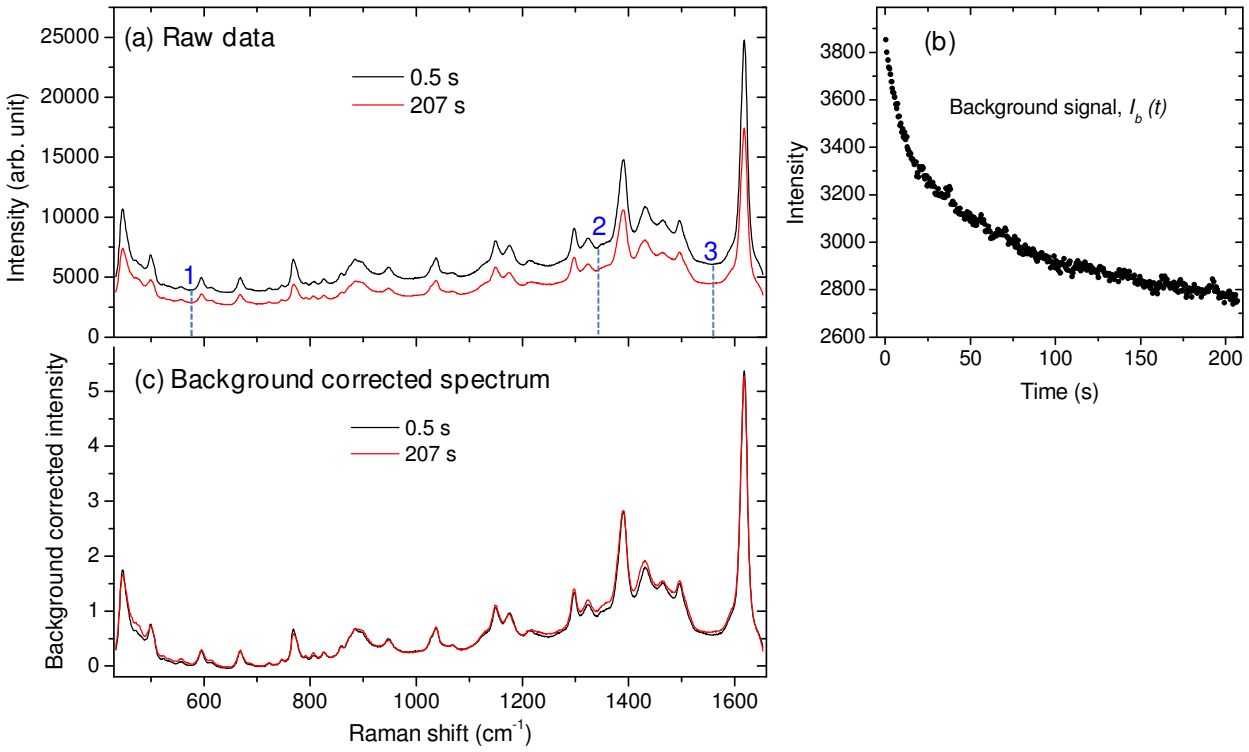

Figure S2 Illustration of background signal change as a function of continuous illumination. (a) Spectra at the beginning of illumination (black line) and after 207 seconds (red line). (b) Time dependence of the background signal where there is no vibrational band (at position ~707 cm^{-1}). The trend is the same if other locations labeled 1, 2 or 3 in (a) are used. (c) The spectra acquired at 0.5 s and 207 s exposure time after background correction.

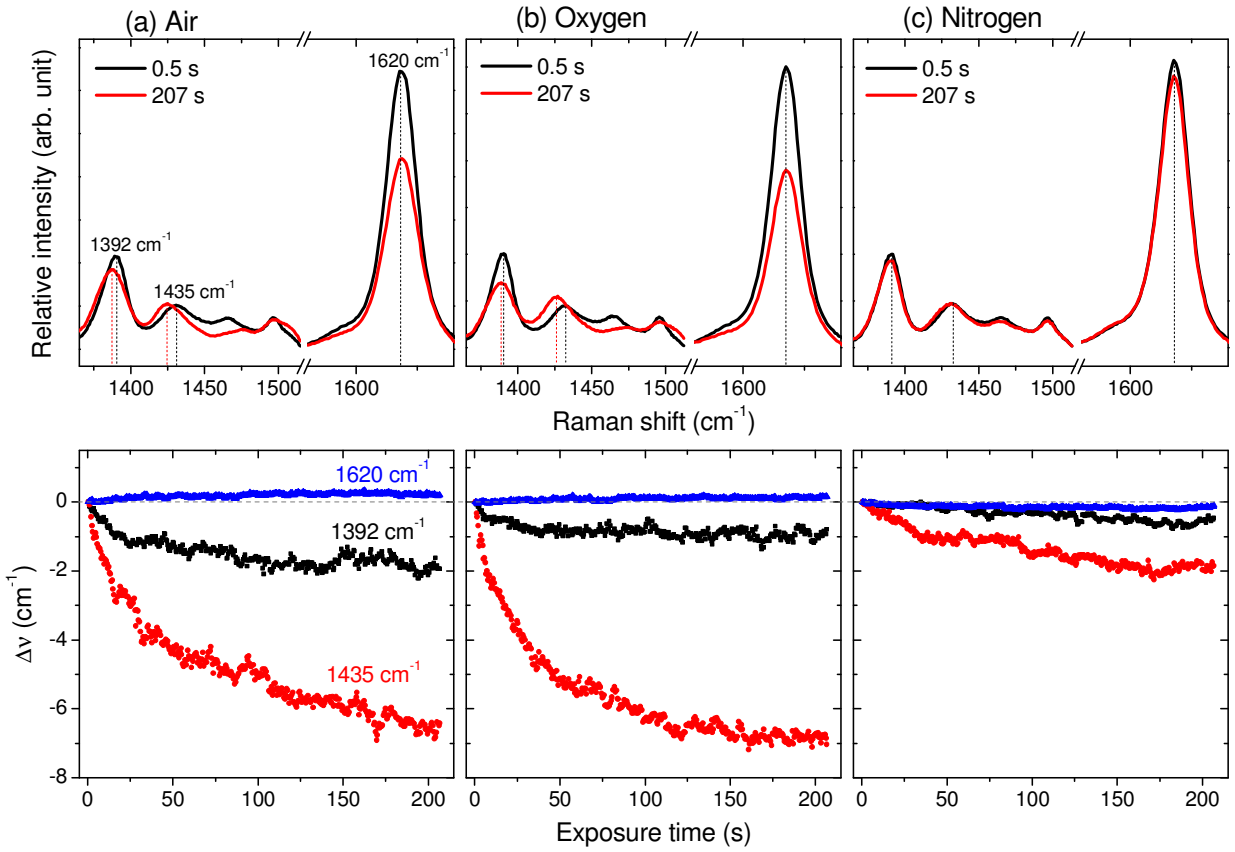

Figure S3 Vibrational frequency shift as a function of exposure time. Top panels: the first (black line) and the last (red line) spectra out of 400 spectra recorded sequentially during the continuous illumination of the MB-AuNR sample for ~207 seconds in (a) air, (b) oxygen and (c) nitrogen atmospheres. Bottom panels: the vibration frequency peak values plotted as a function of exposure time. The peak values are extracted by fitting Gaussian functions to the spectra. Each spectrum is acquired with 0.5 s acquisition time at 633 nm excitation wavelength and 0.4 mW incident laser power.

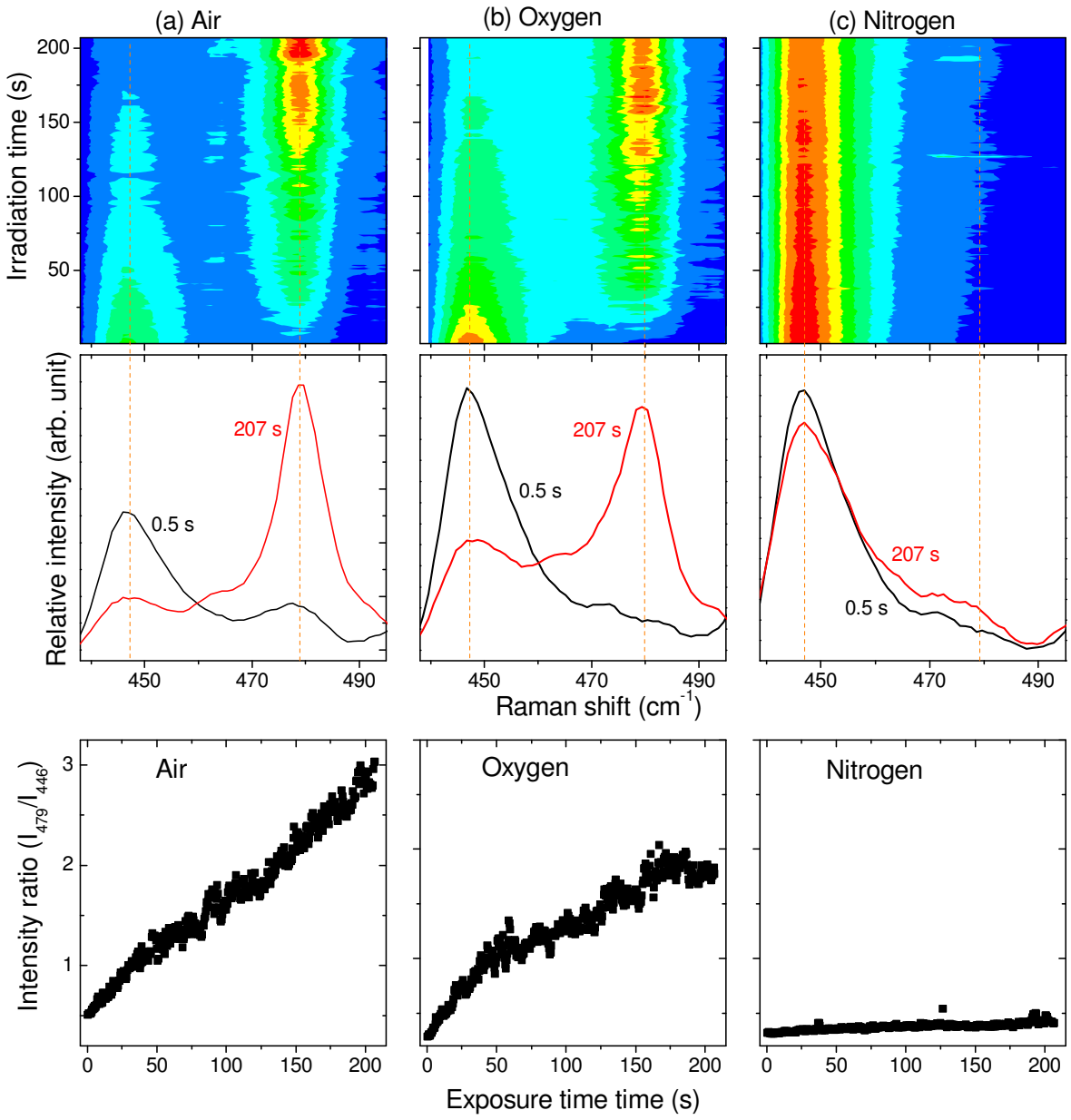

Figure S4 Top panels: Intensity map representing 400 spectra showing the decline of MB reactant signal at 446 cm^{-1} and growth of thionine product signal at 479 cm^{-1} as a function of exposure time in (a) air, (b) oxygen and (c) nitrogen atmospheres. Middle panels: spectra showing the relative intensities of the 446 cm^{-1} (reactant) and 479 cm^{-1} (product) peaks at the beginning (black line) and end (red line) of illumination for 207 seconds in air, oxygen and nitrogen atmospheres. Bottom panels: product to reactant peak intensity ratios in air, oxygen and nitrogen atmospheres.

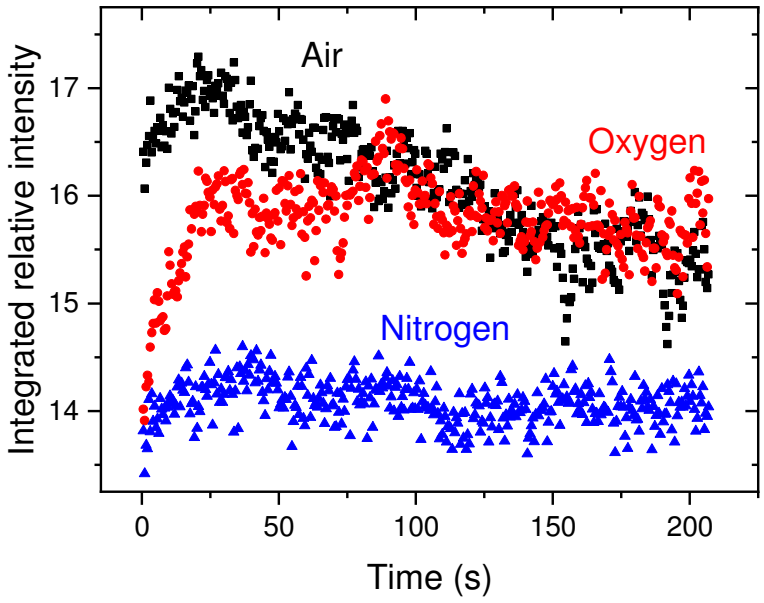

Figure S5 Relative intensity of the 1435 cm^{-1} band as a function of exposure time at 0.4 mW incident laser power and 0.5 s acquisition times. This is enlarged view of the data plotted in Figures 2d-f.

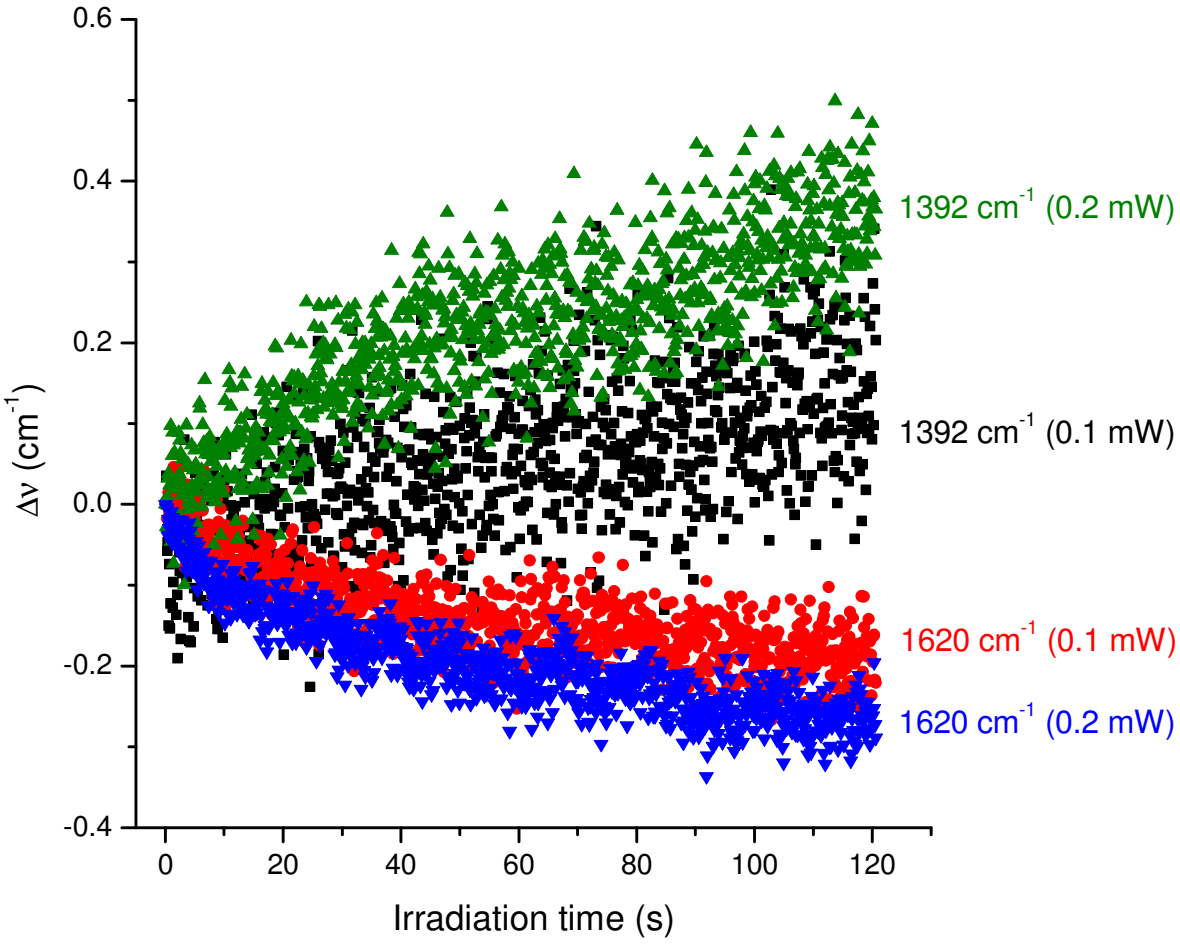

Figure S6 Frequency shift of the 1392 cm^{-1} and 1620 cm^{-1} vibration bands as a function of exposure time in nitrogen atmosphere at different incident laser powers as labeled for a different sample from that used to obtain the data in Figure 3. In each case, the peak values are extracted from 1000 spectra recorded within 120 s continuous exposure time using 0.1 s acquisition time for each spectrum.

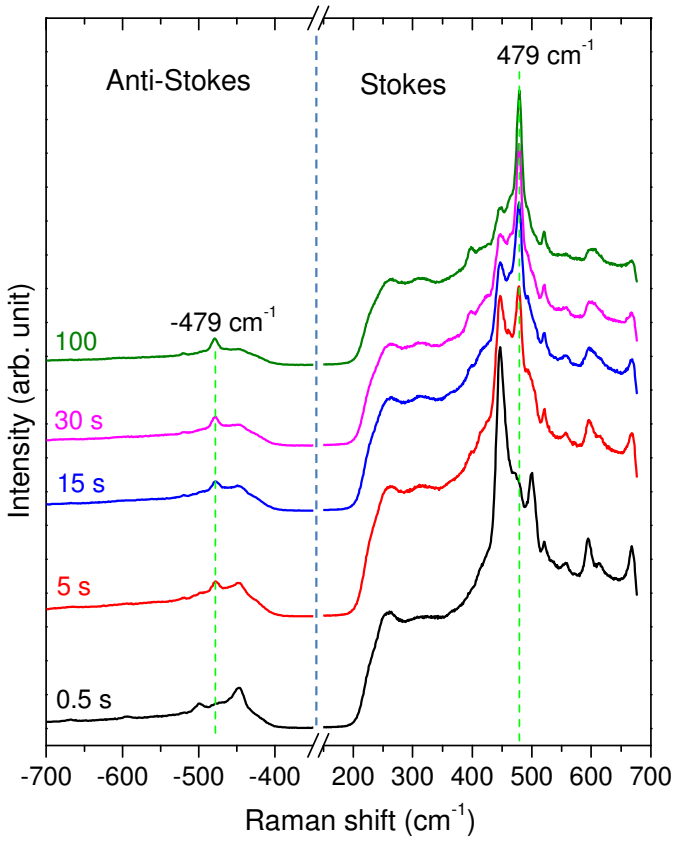

Figure S7 Comparison of Stokes and anti-Stokes Raman scattering intensities obtained at 633 nm excitation wavelength.

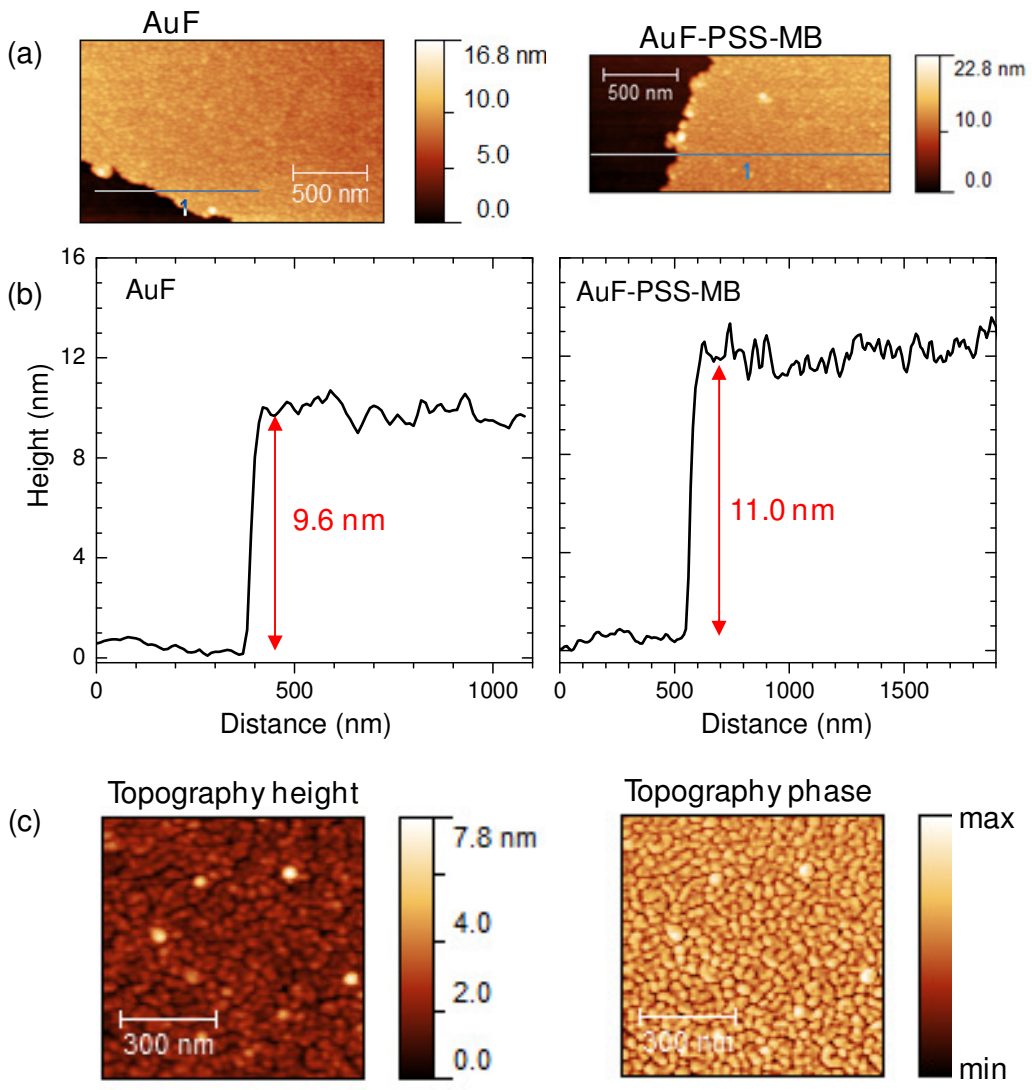

Figure S8 Atomic force microscope (AFM) scan images of gold film prepared by electron-beam evaporation before and after poly(sodium 4-styrenesulfonate) (PSS) coating. (a) AFM topography. The edges are created by scratching the surface with a stainless steel tweezer to determine the height. (b) Profiles along the lines indicated on the images in (a). (C) AFM topography and phase images showing the nanostructures of the gold film with the PSS-MB spacer layer and adsorbate assembly.

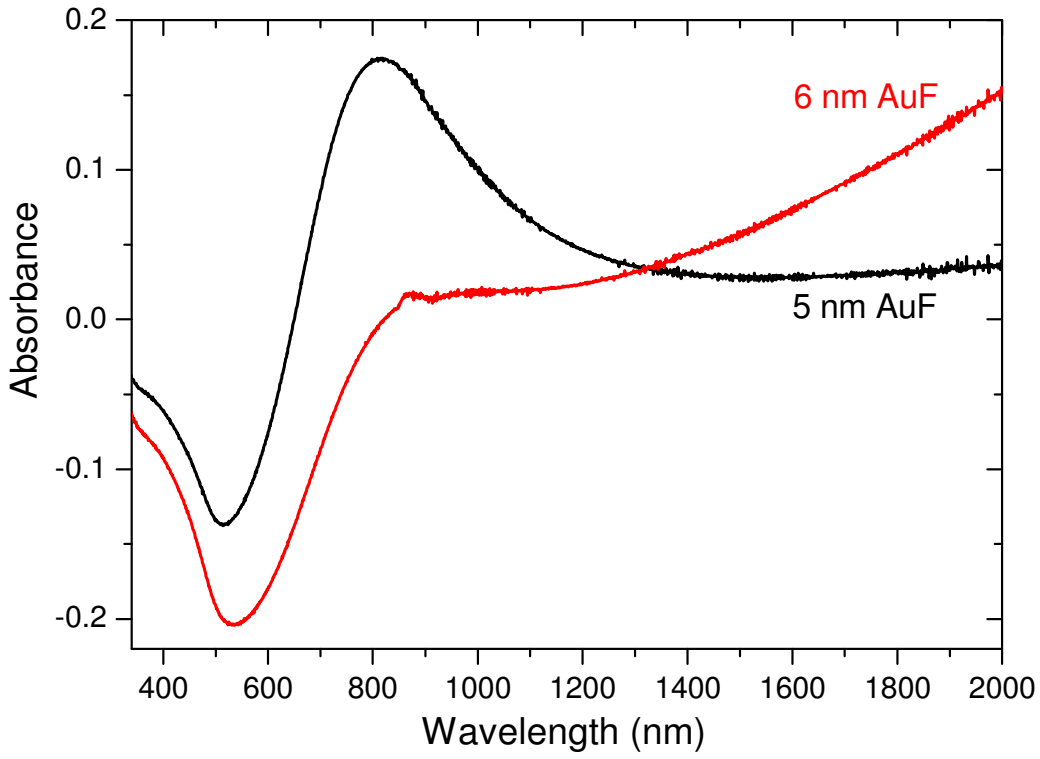

Figure S9 Absorbance of gold films with targeted evaporation thicknesses of 5 nm and 6 nm, which are estimated to be 9 and 10 nm based on AFM measurement as shown in Figure S9. Notice that for the thicker film (red line), the absorption toward the near-infrared wavelength is increasing more rapidly as expected when the film approaches bulk property with increasing thickness.